



Revealing the Underestimation of Anthropogenic Organosulfates in

2	Atmos	pheric	Aerosols	s in	Urban	Region
-	ALIHOS	phonic	1 1 CI USUI	, 111	Olban	116210

- 3 Yanting Qiu^{1#}, Junrui Wang^{1#}, Tao Qiu², Jiajie Li³, Yanxin Bai⁴, Teng Liu¹, Ruiqi Man¹,
- 4 Taomou Zong¹, Wenxu Fang¹, Jiawei Yang¹, Yu Xie¹, Zeyu Feng¹, Chenhui Li³, Ying Wei³,
- 5 Kai Bi⁵, Dapeng Liang², Ziqi Gao⁶, Zhijun Wu^{1,*}, Yuchen Wang^{4,*}, Min Hu¹
- 6 1 State Key Laboratory of Regional Environment and Sustainability, College of
- 7 Environmental Sciences and Engineering, Peking University, Beijing 100871, China;
- 8 ² Key Lab of Groundwater Resources and Environment of the Ministry of Education,
- 9 College of New Energy and Environment, Jilin University, Changchun 130012, China
- 10 ³ College of Environment and Ecology, Laboratory of Compound Air Pollutions
- 11 Identification and Control, Taiyuan University of Technology, Taiyuan, 030024, China
- ⁴ College of Environmental Science and Engineering, Hunan University, Changsha,
- 13 Hunan, 410082, China
- ⁵ Beijing Key Laboratory of Cloud, Precipitation and Atmospheric Water Resources,
- 15 Beijing Meteorological Service, Beijing, China
- ⁶ University of Virginia Environmental Institute, Charlottesville, VA 22902, United States
- 17 #: Yanting Qiu and Junrui Wang contributed equally to this work
- *Correspondence Author:
- 19 Zhijun Wu (zhijunwu@pku.edu.cn) and Yuchen Wang (ywang@hnu.edu.cn)





ABSTRACT

2122

23

24

25

26

2728

29

30

31 32

33

34

35

36 37

38 39

40

Organosulfates (OSs) are important component of organic aerosols, which serve as critical tracers of secondary organic aerosols (SOA). However, molecular composition, classification, and formation driving factors of OSs at different atmospheric conditions have not been fully constrained. In this work, we integrated OSs molecular composition, precursor-constrained positive matrix factorization (PMF) source apportionment, and OSs-precursor correlation analysis to classify OSs detected from PM_{2.5} samples collected from three different cities (Beijing, Taiyuan, and Changsha). This new approach enables the accurate classification of OSs from molecular perspective. Compared with conventional classification methods, we found the mass fraction of Aliphatic OSs and nitrooxy OSs (NOSs) increased by 22.0%, 17.8%, and 10.3% in Beijing, Taiyuan, and Changsha, respectively, highlighting the underestimation of Aliphatic OSs and NOSs in urban regions. The formation driving factors of Aliphatic OSs and NOSs were further investigated. We found that elevated aerosol liquid water content promoted the formation of Aliphatic OSs and NOSs only when aerosols transition from non-liquid state to liquid state. In addition, enhanced inorganic sulfate mass concentrations, and O_x ($O_x = NO_2 +$ O₃) concentrations, as well as decreased aerosol pH commonly facilitated the formation of Aliphatic OSs and NOSs. These results reveal the underestimation of OSs derived from anthropogenic emission, highlighting the potential indicative role of Aliphatic OSs and NOSs in urban SOA.

41 **KEY WORDS**: non-target analysis; high-resolution mass spectrometry; secondary organic aerosol; PMF source apportionment





1. Introduction

Due to the diversity of natural and anthropogenic emissions and the complexity of atmospheric chemistry, investigating the chemical characterization and formation mechanisms of secondary organic aerosols (SOA) remains challenging. Among SOA components, organosulfates (OSs) have emerged as key tracers as their formation is primarily governed by secondary atmospheric processes (Iinuma et al., 2007a; Iinuma et al., 2007b; Surratt et al., 2007; Surratt et al., 2008). Moreover, OSs significantly influence the aerosol physicochemical properties, including acidity (Riva et al., 2019; Zhang et al., 2019), hygroscopicity (Estillore et al., 2016; Ohno et al., 2022; Hansen et al., 2015), and light-absorption properties (Fleming et al., 2019; Jiang et al., 2025). Therefore, a deeper understanding of OS abundances, sources, and formation drivers is crucial for elucidating SOA formation and its properties.

Quantifying OS abundances is vital to assess their contribution to SOA. However, this is difficult due to the large number and structural diversity of OS molecules and the lack of authentic standards. Most studies quantify a few representative OSs using synthetic or surrogate standards (Wang et al., 2020; Wang et al., 2017; Huang et al., 2018b; He et al., 2022), while non-target analysis (NTA) with high-resolution mass spectrometry (HRMS) offers broader molecular characterization (Huang et al., 2023a; Wang et al., 2022b; Cai et al., 2020). Although NTA combined with surrogate standards allows molecular-level (semi-)quantification, overall OS mass concentrations remain underestimated, and many OSs remain unidentified (Lukács et al., 2009; Cao et al., 2017; Tolocka and Turpin, 2012; Ma et al., 2025).

Accurate classification of OSs by their precursors is essential for reliable quantification and mechanistic insights. OSs from specific precursors generally share similar elemental compositions, with characteristic ranges of C atoms, double bond equivalents (DBE), and aromaticity equivalents (Xc). For example, isoprene-derived OSs typically contain 4–5 C atoms; monoterpene- and sesquiterpene-derived OSs usually have 9–10 and 14–15 C atoms, respectively (Lin et al., 2012; Riva et al., 2016b; Wang et al., 2019a; Surratt et al., 2008; Riva et al., 2015). An "OSs precursor map," correlating molecular weight and carbon number based on chamber studies, has been developed to classify OSs accordingly (Wang et al., 2019a). However, these approaches often oversimplify OSs formation by relying solely on elemental composition, leaving many OSs without identified precursors.

The formation mechanisms of OSs remain incompletely understood, though several driving factors have been identified through controlled chamber experiments and ambient observations. For instance, increased aerosol liquid water content (ALWC) enhances OSs formation by promoting the uptake of gaseous precursors (Edwards et al., 2017; Brown et al., 2012). Inorganic sulfate can also affect OSs formation by acting as nucleophiles via epoxide pathway (Eddingsaas et al., 2010; Wang et al., 2020; Cooke et al., 2024). However, meteorological conditions vary across cities, meaning the relative importance of these factors may differ by location. Thus, evaluating these formation drivers under diverse atmospheric conditions is essential. Identifying both common and region-specific drivers is key to a comprehensive understanding of OSs formation mechanisms.

In this study, we employed non-target analysis (NTA) using ultra-high performance liquid chromatography (UHPLC) coupled with high-resolution mass spectrometry (HRMS) to characterize





- OSs molecular composition in PM_{2.5} samples from three cities. Identified OSs were classified by their
- 85 VOCs precursors—including aromatic, aliphatic, monoterpene, and sesquiterpene VOCs—via
- 86 precursor-constrained positive matrix factorization (PMF). Mass concentrations were quantified or
- 87 semi-quantified using authentic or surrogate standards. Additionally, spatial variations in OSs
- 88 concentrations and co-located environmental factors were analyzed to distinguish both common and
- 89 site-specific drivers of OSs formation.

2. Methodology

2.1 Sampling and Filter Extraction

Field observations were conducted during winter (December 2023 to January 2024) at three urban sites: Beijing, Taiyuan, and Changsha. In Beijing, PM_{2.5} samples were collected at the Peking University Atmosphere Environment Monitoring Station (PKUERS; 40.00°N, 116.32°E), as detailed in previous studies (Wang et al., 2023a). Sampling in Taiyuan and Changsha took place on rooftops at the Taoyuan National Control Station for Ambient Air Quality (37.88°N, 112.55°E) and the Hunan Hybrid Rice Research Center (28.20°N, 113.09°E), respectively (see Figure S1).

Daily PM_{2.5} samples were collected on quartz fiber filters (ϕ = 47 mm, Whatman Inc.) from 9:00 to 8:00 local time the next day. In Beijing and Taiyuan, RH-resolved sampling was performed using an RH-resolved sampler, stratifying daily samples into low (RH \leq 40%), moderate (40% \leq RH \leq 60%), and high (RH > 60%) RH regimes. Due to persistently high RH in Changsha, a four-channel sampler (TH-16, Wuhan Tianhong Inc.) collected samples without RH stratification. Consequently, Beijing and Taiyuan collected one or more samples daily, whereas Changsha collected one sample per day. Considering the potential overestimate of monoterpene OSs detected due to the reaction of SO₂ on filters (Brüggemann et al., 2021), a denuder coated with NaCl and Na₂CO₃ was installed upstream of the sampler to remove SO₂. A total of 40, 64, and 30 samples were obtained from Beijing, Taiyuan, and Changsha, respectively. The sampled filters were stored in a freezer at -18 °C, and the duration from sampling to analysis was 40 days. Prior to analysis, all samples were equilibrated for 24 hours under controlled temperature (20 ± 1 °C) and RH (40-45%). Average daily PM_{2.5} mass concentrations and RH during sampling are summarized in Table S1.

Sample extraction followed established protocols (Wang et al., 2020). Briefly, filters were ultrasonically extracted with LC-MS grade methanol (Merck Inc.), filtered through 0.22 μ m PTFE syringe filters, and evaporated under a gentle stream of high-purity N₂ (>99.99%). The dried extracts were then redissolved in 2 mL of LC-MS grade methanol for analysis.

During the campaign, gaseous pollutants (SO₂, NO₂, O₃, CO) were monitored using automatic analyzers. PM_{2.5} and PM₁₀ mass concentrations were measured by tapered element oscillating microbalance (TEOM). Water-soluble ions (Na⁺, NH₄⁺, K+, Mg²⁺, Ca²⁺, Cl⁻, NO₃⁻, SO₄²⁻) were analyzed with the Monitor for AeRosols and Gases in ambient Air (MARGA) coupled with ion chromatography. Organic carbon (OC) and elemental carbon (EC) were quantified by online OC/EC analyzers or carbon aerosol speciation systems. Trace elements in PM_{2.5} were determined by X-ray fluorescence spectrometry (XRF). Additionally, VOCs concentrations were measured using an online





gas chromatography-mass spectrometry (GC-MS) system with a one-hour time resolution in Taiyuan and Changsha. Table S2 summarizes the monitoring instruments deployed at each site.

2.2 Identification of Organosulfates

The molecular composition of PM_{2.5} extracts was analyzed using an ultra-high performance liquid chromatography (UHPLC) system (Thermo Ultimate 3000, Thermo Scientific) coupled with an Orbitrap HRMS (Orbitrap Fusion, Thermo Scientific) equipped with an electrospray ionization (ESI) source operating in negative mode. Chromatographic separation was achieved on a reversed-phase Accucore C18 column (150 × 2.1 mm, 2.6 µm particle size, Thermo Scientific). For tandem MS acquisition, full MS scans (m/z 70–700) were collected at a resolving power of 120,000, followed by data-dependent MS/MS (ddMS²) scans (m/z 50-500) at 30,000 resolving power. Detailed UHPLC-HRMS² parameters are provided in Text S1.

NTA was performed using Compound Discoverer (CD) software (version 3.3, Thermo Scientific) to identify chromatographic peak features (workflow details in Table S3). Molecular formulas were assigned based on elemental combinations $C_cH_hO_oN_nS_s$ (c=1-90, h=1-200, o=0-20, n=0-1, s=1) within a mass tolerance of 0.005 Da. Formulas with hydrogen-to-carbon (H/C) ratios outside 0.3–3.0 and oxygen-to-carbon (O/C) ratios beyond 0–3.0 were excluded to remove implausible assignments. Double bound equivalent (DBE) and Xc (Ma et al., 2022) were calculated using eqs. (1) and (2), where m and k were the fractions of oxygen and sulfur atoms in the π -bond structures of a compound (both m and k were presumed to be 0.50 in this work (Yassine et al., 2014)).

```
141 DBE = c - 0.5h + 0.5n + 1 (1)
```

 $Xc = (3 \times (DBE - m \times o - k \times s) - 2)/(DBE - m \times o - k \times s)$ (if $DBE < (m \times o + 143 + k \times s)$ or Xc < 0, then Xc was set to 0) (2)

OSs were selected based on compounds with O/S \geq 4 and HSO₄⁻ (m/z 96.96010) and/or SO₃⁻ (m/z 79.95736) fragments were observed in their corresponding MS² spectra. Among them, if N number is 1, O/S \geq 7, and their MS² spectra showed ONO₂⁻ (m/z 61.98837) fragment, these OSs were defined as nitrooxy OSs (NOSs).

2.3 Classification and Quantification/Semi-quantification of Organosulfates

Due to reversed-phase column limitations, concentration estimates of small OSs ($C \le 7$) are highly uncertain (Liu et al., 2024); thus, only OSs with $C \ge 8$ were analyzed. Firstly, we used conventional classification approach following previous studies (Zhao et al., 2018; Wang et al., 2021; Deng et al., 2021; Xu et al., 2021; Mutzel et al., 2015; Brüggemann et al., 2020; Yang et al., 2024; Duporté et al., 2020; Huang et al., 2023b; Wang et al., 2022b; Riva et al., 2016a). All detected OSs and NOSs were classified into seven groups: Monoterpene OSs and NOSs, Aliphatic OSs, Aromatic OSs and NOSs, and Sesquiterpene OSs and NOSs (Table S4). NOSs from aliphatic precursors were not observed. Those without identified precursors were labeled Unknown OSs or NOSs.

Synthetic α -pinene OSs ($C_{10}H_{17}O_5S^{\circ}$) and NOSs ($C_{10}H_{16}NO_7S^{\circ}$) served for (semi-)quantifying Monoterpene and Sesquiterpene OSs and NOSs. Their detailed synthesis procedure was described in previous study (Wang et al., 2019b). Potassium phenyl sulfate ($C_6H_5O_4S^{\circ}$) and sodium octyl sulfate ($C_8H_{17}O_4S^{\circ}$) were used for Aromatic OSs and NOSs and Aliphatic OSs due to lack of authentic





standards (Yang et al., 2023; He et al., 2022; Staudt et al., 2014). Unknown OSs and NOSs were semi-quantified by surrogates with similar retention times (RT) (Yang et al., 2023; Huang et al., 2023b). Table 1 lists the standards, retention times, and quantified categories. Unknown OSs and NOSs were absent between 2.00–5.00 min and after 13.60 min.

Table 1 Chemical structure, UHPLC retention time, and quantified categories of standards used in the quantification/semi-quantification of OSs and NOSs

Formula (M-H)	m/z ([M-H] ⁻)	Chemical structure	UHPLC RT (min)	Quantified OSs categories	
C ₆ H ₅ O ₄ S ⁻	172.99140	OSO3*	0.92	Aromatic OSs and NOSs, Unknown OSs and NOSs (RT 0.50-2.00 min)	
$C_8H_{17}O_4S^-$	209.08530	₩ ₇ 0503-	10.30	Aliphatic OSs, Unknown OSs and NOSs (RT 10.00- 13.60 min)	
$C_{10}H_{17}O_5S^-$	249.08022	OH OSO3	7.73	Monoterpene OSs, Sesquiterpene OSs, Unknown OSs and NOSs (RT 5.00-10.00 min)	
$C_{10}H_{16}NO_7S^{\text{-}}$	294.06530	O ₂ NO OSO ₃	9.26	Monoterpene NOSs and Sesquiterpene NOSs	

To classify the Unknown OSs and NOSs, we first calculated the Xc of each specie. Those with DBE > 2 and Xc > 2.50 were designated as Aromatic OSs and NOSs (Yassine et al., 2014). Subsequently, constrained positive matrix factorization (PMF) analysis was performed using EPA PMF 5.0. Several OSs with known precursors served as auxiliary tracers to guide source apportionment. Specifically, C₁₁H₂₂O₅S and C₁₂H₂₄O₅S for long-chain aliphatic OSs (Yang et al., 2024); C₁₀H₁₀O₇S and C₁₁H₁₄O₇S for Aromatic OSs and NOSs (Riva et al., 2015); C₁₀H₁₈O₅S and C₁₀H₁₇NO₇S for Monoterpene OSs and NOSs, respectively (Surratt et al., 2008; Iinuma et al., 2007a); C₁₄H₂₈O₆S and C₁₅H₂₅NO₇S for Sesquiterpene OSs and NOSs, respectively (Wang et al., 2022b). These were selected due to their high detection frequency (>85%) and the highest average concentrations within their categories. Typical VOCs markers (isoprene, benzene, toluene, styrene, n-dodecane) were also included in the PMF model. Based on marker species, Unknown OSs and NOSs were further categorized into eight groups: Monoterpene, Aromatic, Aliphatic, and Sesquiterpene OSs and NOSs.

Correlation coefficients between classified OSs/NOSs and corresponding VOCs (Monoterpene OSs and NOSs vs. isoprene; Aromatic OSs and NOSs vs. benzene; Aliphatic OSs and NOSs vs. n-dodecane; Sesquiterpene OSs and NOSs vs. isoprene) were calculated, excluding species with R < 0.40. Given monoterpenes and sesquiterpenes primarily originate from biogenic sources and strongly correlate with isoprene (Guenther et al., 2006; Sakulyanontvittaya et al., 2008). Therefore, we checked the relationship between Monoterpene OSs and NOSs, Sesquiterpene OSs and NOSs, and isoprene.

To validate classification accuracy, MS² fragment patterns were analyzed (Table S5). Diagnostic fragments supported the assignments: Aliphatic OSs and NOSs showed sequential alkyl chain





cleavages ($\Delta m/z = 14.0157$) and saturated alkyl fragments ($[C_nH_{2n+1}]^-$ or $[C_nH_{2n-1}]^-$); Monoterpene OSs and NOSs displayed $[C_nH_{2n-3}]^-$ fragments; Aromatic OSs/NOSs exhibited characteristic aromatic substituent fragments ($[C_0H_2R-H]^-$, R =alkyl, carbonyl, -OH, or H). These fragment patterns confirm the reliability of our classification approach.

3. Results and Discussion

3.1 Concentrations, Compositions, and Classification of Organosulfates

Figure 1 shows the temporal variations of OSs and organic aerosols (OA) mass concentrations, as well as RH, during the sampling period across the three cities. The mean OSs concentrations were (41.11 \pm 34.47) ng/m³ in Beijing, (57.39 \pm 39.23) ng/m³ in Taiyuan, and (102.06 \pm 80.54) ng/m³ in Changsha. Table S6 summarizes the average concentrations of PM_{2.5}, OC, gaseous pollutants, OSs mass concentrations, and the mean meteorological parameters during sampling period for all three cities. OSs accounted for 0.64% \pm 0.44%, 0.41% \pm 0.24%, and 0.76% \pm 0.34% of the total OA in Beijing, Taiyuan, and Changsha, respectively.

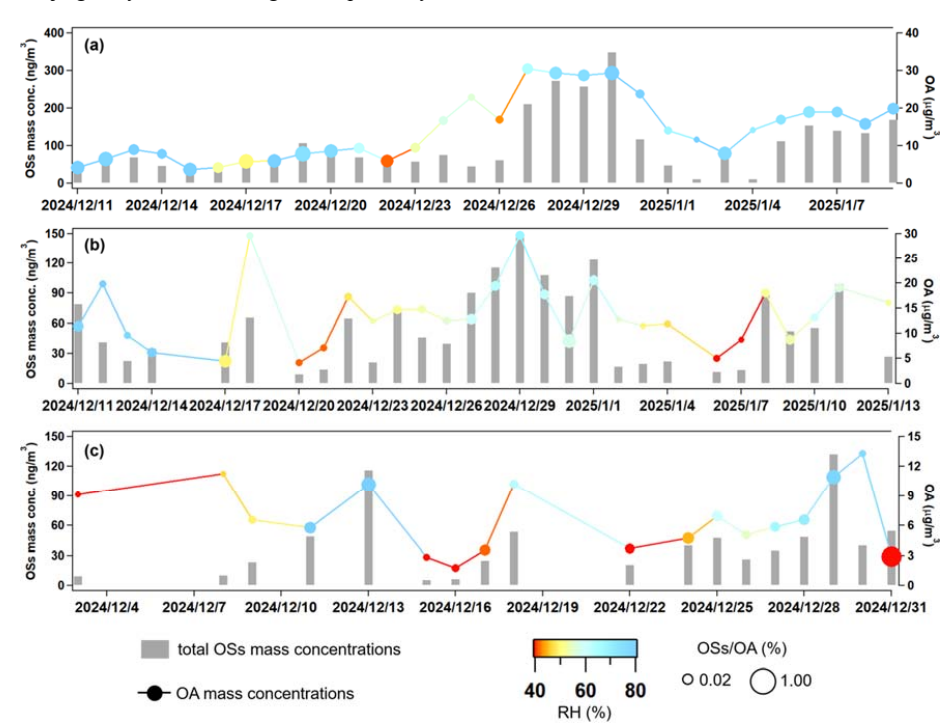


Figure 1 Temporal variations of daily total OSs mass concentrations and average OA mass concentrations in (a) Changsha, (b) Taiyuan, and (c) Beijing. The markers of OA mass concentrations are colored by average RH during sampling period, and marker sizes indicate the OSs/OA mass concentration ratios.

The highest OSs mass concentrations and OSs/OA ratios were observed in Changsha. As shown





in Figure 1(a), a distinct episode with OSs mass concentrations exceeding 300 ng/m³ occurred between December 27th and 31st, leading to the elevated OSs mass concentrations in Changsha. During this period, RH remained consistently above 70%, and the resulting increase in ALWC facilitated OSs formation through aqueous-phase reactions (Cheng et al., 2016b; Wu et al., 2018; Zheng et al., 2015). Furthermore, as shown in Figure S2, concentrations of Ba and K—tracers for fireworks emissions—were elevated, indicating intense fireworks activity. The high ALWC accelerated the heterogeneous conversion of SO₂ from fireworks into particulate sulfate (Figure S3), further promoting OSs formation (Xu et al., 2024; Wang et al., 2020). Additionally, transition metals such as Fe and Mn, emitted during fireworks combustion (Figure S2), catalyzed OSs formation (Huang et al., 2019; Huang et al., 2018a). Collectively, these factors contributed to the pronounced OSs mass concentration observed during this period.

Figures 2(a) and 2(b) shows the average mass concentrations and fractions of different OSs categories across the three cities, based on conventional and our new classification approach, respectively. As displayed in Figure 2(b), Monoterpene OSs and NOSs dominated detected OSs across all cities, contributing 55.2%, 46.8%, and 72.3% to total OSs, respectively. Biogenic-emitted monoterpene is the precursor of Monoterpene OSs and NOSs. However, monoterpenes are primarily biogenic precursors, their limited emissions during winter cannot fully explain the high mass fractions of Monoterpene OSs and NOSs. Recent studies have highlighted anthropogenic sources, particularly biomass burning, as significant contributors to monoterpene (Wang et al., 2022a; Koss et al., 2018). The PM_{2.5} source apportionment analysis (Text S2, Figure S4) confirmed that biomass burning substantially contributed to PM_{2.5} across all cities. The highest total mass fractions of Monoterpene OSs and NOSs in Changsha are mainly attributed to the high RH (Table S6), which facilitates their formation via heterogeneous reactions (Hettiyadura et al., 2017; Wang et al., 2018; Ding et al., 2016a; Ding et al., 2020).

In Taiyuan, the total mass fractions of Aromatic OSs and NOSs (21.2%) were significantly higher than those in Beijing (10.7%) and Changsha (4.6%). Aromatic OSs and NOSs primarily formed via aqueous-phase reactions between S(IV) and aromatic VOCs (Huang et al., 2020). Taiyuan exhibited the highest sulfate mass concentration among the three cities (Table S6), which promoted the formation of these species. Additionally, transition metal ions—particularly Fe³⁺—catalyze aqueous-phase formation of Aromatic OSs and NOSs (Huang et al., 2020). High Fe mass concentration was observed in Taiyuan (0.79 µg/m³), further facilitated the formation of Aromatic OSs and NOSs.

The highest total mass fractions of Aliphatic OSs and NOSs was observed in Beijing (28.1%). The formation mechanisms of Aliphatic OSs and NOSs still remains highly uncertainty up to now. Potential pathways include heterogeneous reactions between SO₂ and alkenes (Passananti et al., 2016), as well as reactions between sulfate and photooxidation products of alkenes (Riva et al., 2016c). Their precursors, mainly long-chain alkenes, are predominantly emitted from fossil fuel combustion and vehicle emissions (He et al., 2022; Wang et al., 2021; Riva et al., 2016c; Tao et al., 2014; Tang et al., 2020). Since fossil fuel combustion and vehicle emissions substantially contributed to PM_{2.5} in all cities (Figure S4), it is suggested that relatively low anthropogenic emissions and low RH promote the dominance of Aliphatic OSs and NOSs. Specifically, low anthropogenic emissions reduce the precursor concentrations for Monoterpene OSs/NOSs and Aromatic OSs/NOSs, while low RH limits their formation through aqueous-phase reactions.



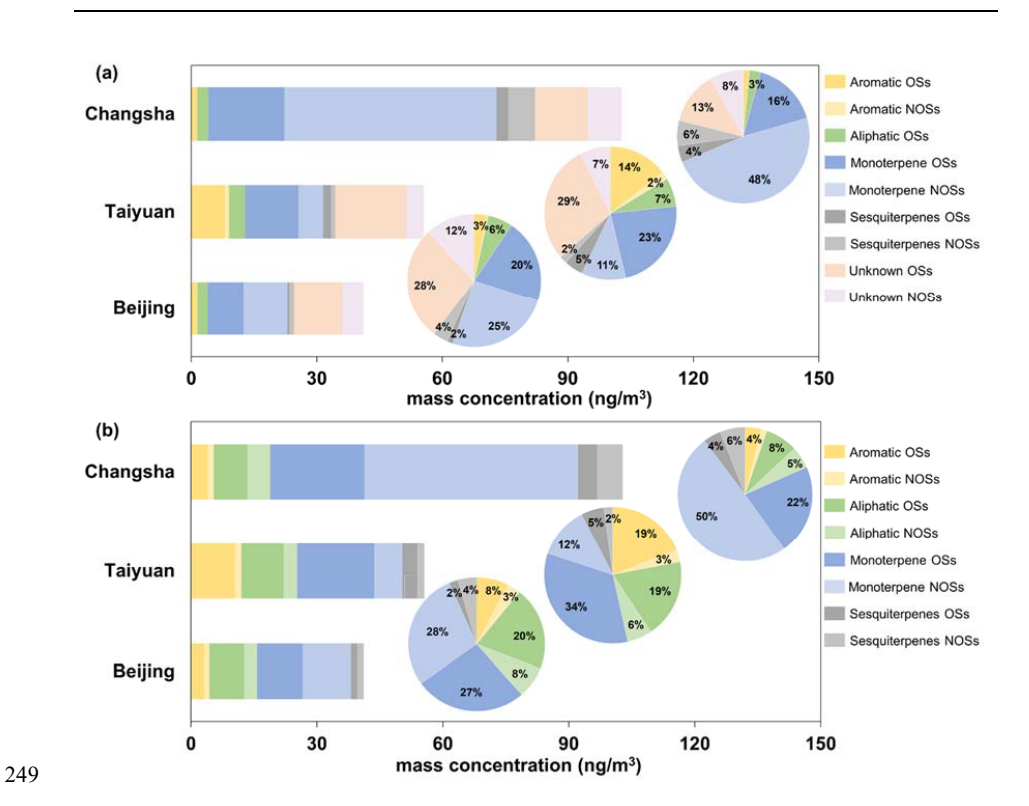


Figure 2 The average mass concentrations of different OSs categories (a) before and (b) after classification across three cities. The inserted pie chart indicates the average mass fractions of different OSs categories.

3.2 Formation Driving Factors of Aliphatic OSs and NOSs

Compared with conventional classification approach (Figure 1(a)), we found Aliphatic OSs and NOSs increased markedly—by 22.0%, 17.8%, and 10.3% in Beijing, Taiyuan, and Changsha, respectively—with Aliphatic NOSs newly identified. Therefore, we further examined the formation drivers of Aliphatic OSs and NOSs.

ALWC plays a key role in facilitate OSs formation (Wang et al., 2020). Using PM_{2.5} chemical composition and RH, ALWC was calculated via the ISORROPIA-II model (details in Text S3) (Fountoukis and Nenes, 2007). Given the direct influence of ambient RH on ALWC (Figure S5) (Bateman et al., 2014) and leveraging RH-resolved samples from Beijing and Taiyuan, we assessed RH effects on Aliphatic OSs/NOSs under low (RH < 40%), medium (40% \leq RH < 60%), and high (RH \geq 60%) conditions.

In Changsha, where RH remains consistently high, Aliphatic OSs and NOSs mass concentrations strongly correlated with RH (R = 0.78). In Beijing and Taiyuan, correlations increased from low to medium RH (Beijing: 0.53 to 0.82; Taiyuan: 0.38 to 0.77) but declined slightly at higher RH (Beijing: 0.82 to 0.69; Taiyuan: 0.77 to 0.72). The initial correlation rise reflects ALWC-enhanced sulfate-driven heterogeneous OSs formation (Wang et al., 2016; Cheng et al., 2016a), while the decline at elevated



269 RH is unexplained.

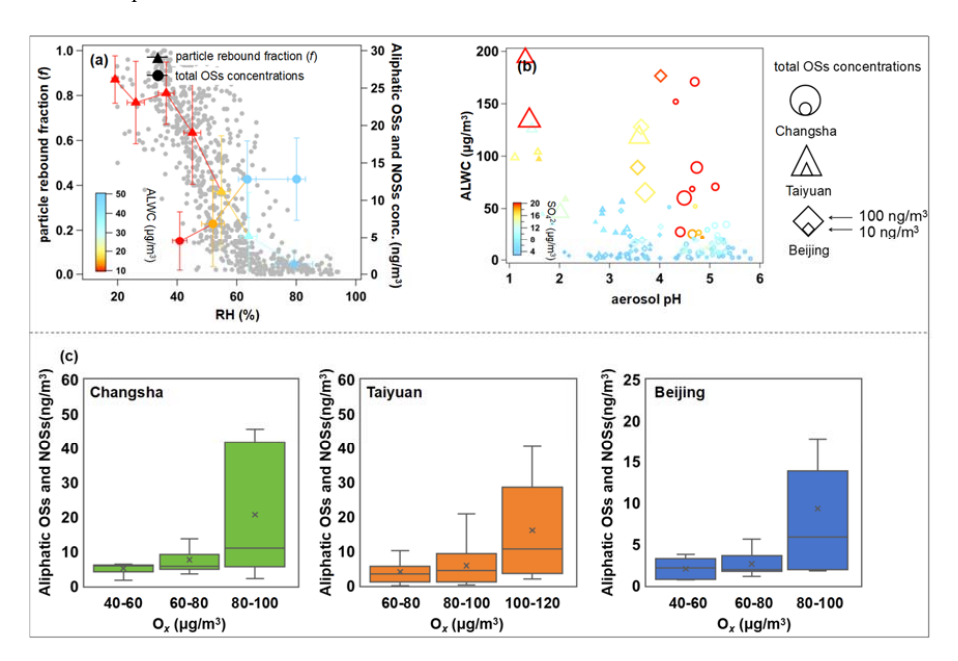


Figure 3 (a) The measured particle rebound fraction (f) and total mass concentrations of Aliphatic OSs and NOSs as a function of RH, the plots were colored by the calculated ALWC concentrations in Taiyuan; (b) the relationship between aerosol pH and ALWC across three cities, the markers were colored by the inorganic sulfate mass concentrations, the marker sizes represented the total mass concentrations of Aliphatic OSs and NOSs; (c) the box plot of total mass concentrations of Aliphatic OSs and NOSs at different O_x concentration levels.

This threshold behavior aligns with aerosol phase transitions. Particle rebound fraction (f), indicating phase state, was measured in Taiyuan using a three-arm impactor (Liu et al., 2017). As RH exceeded 60%, f dropped below 0.2 (Figure 3(a)), signaling a transition from non-liquid to liquid aerosol states. This transition at RH > 60% aligns with prior field (Liu et al., 2017; Liu et al., 2023; Meng et al., 2024; Song et al., 2022)and modeling (Qiu et al., 2023)studies in Eastern China. Correspondingly, Aliphatic OSs and NOSs concentrations increased with RH below 60% but plateaued beyond that despite further humidity rises. These findings underscore aerosol phase state as a critical factor: initial liquid phase formation (RH < 60%) promotes heterogeneous OSs formation (Ye et al., 2018), whereas at higher RH, saturation of reactive interfaces limits further ALWC effects.

In addition, the increase in ALWC with rising RH altered aerosol pH (Figure 3(b)), which inhibited OSs formation via acid-catalyzed reactions (Duporté et al., 2016). In Changsha, as aerosol pH increased from below 1.0 to above 3.0, the average total mass concentrations of Aliphatic OSs and NOSs decreased significantly from 9.3 to 4.6 ng/m³ (Figure S6), with further declines as pH increased. In Taiyuan, OS concentrations dropped from 12.2 to 6.8 ng/m³ as pH rose from below 4.5 to above 5.0. However, in Beijing, total mass concentrations of Aliphatic OSs and NOSs remained stable within a narrow pH range of 3.2–3.9. Elevated ALWC facilitates aqueous-phase radical chemistry that forms





OSs via non-acid pathways, which can dominate over pH-dependent processes (Rudziński et al., 2009; Wach et al., 2019; Huang et al., 2019). Thus, pH-dependent suppression of aliphatic OSs and NOSs formation is common across urban aerosol pH ranges, but less evident when pH varies narrowly.

Inorganic sulfate plays a crucial role in OSs formation via sulfate esterification reactions (Xu et al., 2024; Wang et al., 2020). We thus examined its effect on the formation of Aliphatic OSs and NOSs. Figure 3(b) illustrates the relationships among ALWC, pH, inorganic sulfate mass concentration, and total mass concentrations of Aliphatic OSs and NOSs across all cities. A consistent positive correlation was observed, consistent with previous field studies (Lin et al., 2022; Wang et al., 2023b; Le Breton et al., 2018; Wang et al., 2018). This correlation was strongest when sulfate concentrations were below 20 µg/m³. Below this threshold, total mass concentrations of Aliphatic OSs and NOSs increased significantly with inorganic sulfate, whereas above it, the correlation weakened. Additionally, inorganic sulfate mass concentration showed a clear positive correlation with ALWC (Figure 3(b)), suggesting that ionic strength did not increase linearly with sulfate mass. This likely reflects saturation effects in acid-mediated pathways, driven by limitations in water activity and ionic strength (Wang et al., 2020). Overall, these results highlight the nonlinear influence of inorganic sulfate on Aliphatic OSs and NOSs formation.

Atmospheric oxidative capacity, represented by O_x ($O_x = O_3 + NO_2$) concentrations, typically modulates OSs formation via acid-catalyzed ring-opening reactions pathways. As shown in Figure 3(c), total mass concentrations of Aliphatic OSs and NOSs exhibited significant increases with rising O_x levels across all cities. Especially, total mass concentrations of Aliphatic OSs and NOSs significantly increased across all cities when O_x concentrations raised from $60-80 \,\mu\text{g/m}^3$ to $> 80 \,\mu\text{g/m}^3$. As shown in Figure S7, O_3 dominated the O_x composition during high- O_x episodes ($> 80 \,\mu\text{g/m}^3$) across all cities. Therefore, we inferred that high O_x conditions enhance the oxidation of VOCs (Zhang et al., 2022; Wei et al., 2024), leading to heterogeneous Aliphatic OSs and NOSs formation via acid-catalyzed ring-opening reactions pathways (Eddingsaas et al., 2010; Iinuma et al., 2007a; Brüggemann et al., 2020).

4 Conclusions and Implications

In this study, we applied a non-target analysis (NTA) approach based on UHPLC-HRMS to investigate the molecular composition of OSs in PM_{2.5} samples from three cities. By integrating molecular composition data, precursor-constrained PMF source apportionment, and OSs-precursor correlation analysis, we developed a comprehensive method for accurate classification of detected OSs, demonstrating superior discrimination between aliphatic OSs and nitrogen-containing OSs (NOSs). Conventional classification methods rely on laboratory chamber-derived precursor-OSs relationships (Wang et al., 2019a), which provide limited insight into the formation of aliphatic OSs and NOSs and tend to underestimate their mass fractions. The abundant Aliphatic OSs and NOSs detected in ambient PM_{2.5} suggest complex formation pathways, such as OH oxidation of long-chain alkenes (Riva et al., 2016c) and heterogeneous SO₂-alkene reactions in acidic environments (Passananti et al., 2016), which remain incompletely understood in laboratory studies. Our findings highlight the importance of emphasizing the formation of Aliphatic OSs and NOSs in urban atmospheres.

https://doi.org/10.5194/egusphere-2025-4549 Preprint. Discussion started: 5 November 2025 © Author(s) 2025. CC BY 4.0 License.





333 However, this approach depends on public molecular composition datasets, potentially 334 underestimating OSs mass concentrations in urban environments. For example, OSs identified here 335 accounted for less than 1% of total OA mass, whereas recent work (Ma et al., 2025) reported 336 approximately 20% contributions. Furthermore, OSs may become increasingly significant in OA, 337 particularly in coastal regions influenced by oceanic dimethyl sulfate emissions (Brüggemann et al., 338 2020). Future work will focus on synthesizing OSs standards representing various precursors and 339 establishing a dedicated fragmentation database through multi-platform MS² validation to elucidate 340 OSs sources in more detail. 341 **Author Contributions** 342 Y.Q., J.W., and Z.W. designed this work. J.L., Y.Wei, C.L., J.Y., T.L., R.M., T.Z., W.F., J.Y., Z.F., Y.X. and K.B. collected PM2.5 samples. Y.Q., J.W., T.Q., Y.B., and D.L. conducted UHPLC-HRMS 343 344 experiments. Y.Q., J.W., Z.G., and Y.Wang wrote this manuscript. Z.W., Y.Wang, and M.H. edited this 345 manuscript. All authors have read and agreed to submit this manuscript. Y.Q. and J.W. contributed 346 equally to this work. 347 **Funding** 348 This work is funded by Young Scientists Fund of the National Nature Science Foundation of China 349 (Grants 22306059), This work was also supported by the Science and Technology Innovation 350 Program of Hunan Province (Grants 2024RC3106 and 2025AQ2001), and the Fundamental Research Funds for the Central Universities (Grant 531118010830). 351 352 Notes 353 The authors declare that they have no conflict of interest. 354 Acknowledgements 355 Y.W would like to acknowledge financial support by the Young Scientists Fund of the National 356 Nature Science Foundation of China (Grants 22306059), This work was also supported by the Science and Technology Innovation Program of Hunan Province (Grants 2024RC3106 and 357 358 2025AQ2001), and the Fundamental Research Funds for the Central Universities (Grant

359360

531118010830).





References

- 362 Bateman, A. P., Belassein, H., Martin, S. T.: Impactor Apparatus for the Study of Particle Rebound:
- 363 Relative Humidity and Capillary Forces. Aerosol Science and Technology. 48, 42-52.
- 364 10.1080/02786826.2013.853866, 2014.
- Brown, S. S., Dubé, W. P., Karamchandani, P., Yarwood, G., Peischl, J., Ryerson, T. B., Neuman, J. A.,
- 366 Nowak, J. B., Holloway, J. S., Washenfelder, R. A., Brock, C. A., Frost, G. J., Trainer, M., Parrish, D. D.,
- 367 Fehsenfeld, F. C., Ravishankara, A. R.: Effects of NOx control and plume mixing on nighttime chemical
- 368 processing of plumes from coal-fired power plants. Journal of Geophysical Research: Atmospheres. 117.
- 369 https://doi.org/10.1029/2011JD016954, 2012.
- 370 Brüggemann, M., Xu, R., Tilgner, A., Kwong, K. C., Mutzel, A., Poon, H. Y., Otto, T., Schaefer, T.,
- 371 Poulain, L., Chan, M. N., Herrmann, H.: Organosulfates in Ambient Aerosol: State of Knowledge and
- 372 Future Research Directions on Formation, Abundance, Fate, and Importance. Environmental Science &
- 373 Technology. 54, 3767-3782. 10.1021/acs.est.9b06751, 2020.
- 374 Brüggemann, M., Riva, M., Perrier, S., Poulain, L., George, C., Herrmann, H.: Overestimation of
- 375 Monoterpene Organosulfate Abundance in Aerosol Particles by Sampling in the Presence of SO2.
- Environmental Science & Technology Letters. 8, 206-211. 10.1021/acs.estlett.0c00814, 2021.
- 377 Cai, D., Wang, X., Chen, J., Li, X.: Molecular Characterization of Organosulfates in Highly Polluted
- 378 Atmosphere Using Ultra-High-Resolution Mass Spectrometry. Journal of Geophysical Research:
- 379 Atmospheres. 125, e2019JD032253. https://doi.org/10.1029/2019JD032253, 2020.
- 380 Cao, G., Zhao, X., Hu, D., Zhu, R., Ouyang, F.: Development and application of a quantification
- method for water soluble organosulfates in atmospheric aerosols. Environmental Pollution. 225, 316-322.
- 382 <u>https://doi.org/10.1016/j.envpol.2017.01.086</u>, 2017.
- Cheng, Y., Zheng, G., Wei, C., Mu, Q., Zheng, B., Wang, Z., Gao, M., Zhang, Q., He, K., Carmichael,
- 384 G., Pöschl, U., Su, H.: Reactive nitrogen chemistry in aerosol water as a source of sulfate during haze events
- 385 in China. 2, e1601530. doi:10.1126/sciadv.1601530, 2016a.
- 386 Cheng, Y., Zheng, G., Wei, C., Mu, Q., Zheng, B., Wang, Z., Gao, M., Zhang, Q., He, K., Carmichael,
- 387 G., Pöschl, U., Su, H.: Reactive nitrogen chemistry in aerosol water as a source of sulfate during haze events
- 388 in China. Science Advances. 2, e1601530. 10.1126/sciadv.1601530, 2016b.
- Cooke, M. E., Armstrong, N. C., Fankhauser, A. M., Chen, Y., Lei, Z., Zhang, Y., Ledsky, I. R., Turpin,
- 390 B. J., Zhang, Z., Gold, A., McNeill, V. F., Surratt, J. D., Ault, A. P.: Decreases in Epoxide-Driven Secondary
- 391 Organic Aerosol Production under Highly Acidic Conditions: The Importance of Acid-Base Equilibria.
- 392 Environmental Science & Technology. 58, 10675-10684. 10.1021/acs.est.3c10851, 2024.
- Deng, Y., Inomata, S., Sato, K., Ramasamy, S., Morino, Y., Enami, S., Tanimoto, H.: Temperature and
- 394 acidity dependence of secondary organic aerosol formation from α-pinene ozonolysis with a compact
- 395 chamber system. Atmos. Chem. Phys. 21, 5983-6003. 10.5194/acp-21-5983-2021, 2021.
- 396 Ding, X., He, Q.-F., Shen, R.-Q., Yu, Q.-Q., Zhang, Y.-Q., Xin, J.-Y., Wen, T.-X., Wang, X.-M.: Spatial
- 397 and seasonal variations of isoprene secondary organic aerosol in China: Significant impact of biomass





- burning during winter. Scientific Reports. 6, 20411. 10.1038/srep20411, 2016a.
- 399 Ding, X., Zhang, Y.-Q., He, Q.-F., Yu, Q.-Q., Shen, R.-Q., Zhang, Y., Zhang, Z., Lyu, S.-J., Hu, Q.-H.,
- 400 Wang, Y.-S., Li, L.-F., Song, W., Wang, X.-M.: Spatial and seasonal variations of secondary organic aerosol
- 401 from terpenoids over China. Journal of Geophysical Research: Atmospheres. 121, 14,661-614,678.
- 402 https://doi.org/10.1002/2016JD025467, 2016b.
- Duporté, G., Flaud, P. M., Geneste, E., Augagneur, S., Pangui, E., Lamkaddam, H., Gratien, A.,
- 404 Doussin, J. F., Budzinski, H., Villenave, E., Perraudin, E.: Experimental Study of the Formation of
- 405 Organosulfates from α-Pinene Oxidation. Part I: Product Identification, Formation Mechanisms and Effect
- 406 of Relative Humidity. The Journal of Physical Chemistry A. 120, 7909-7923. 10.1021/acs.jpca.6b08504,
- 407 2016.
- 408 Duporté, G., Flaud, P. M., Kammer, J., Geneste, E., Augagneur, S., Pangui, E., Lamkaddam, H.,
- 409 Gratien, A., Doussin, J. F., Budzinski, H., Villenave, E., Perraudin, E.: Experimental Study of the Formation
- 410 of Organosulfates from α-Pinene Oxidation. 2. Time Evolution and Effect of Particle Acidity. The Journal
- 411 of Physical Chemistry A. 124, 409-421. 10.1021/acs.jpca.9b07156, 2020.
- 412 Eddingsaas, N. C., VanderVelde, D. G., Wennberg, P. O.: Kinetics and Products of the Acid-Catalyzed
- 413 Ring-Opening of Atmospherically Relevant Butyl Epoxy Alcohols. The Journal of Physical Chemistry A.
- 414 114, 8106-8113. 10.1021/jp103907c, 2010.
- 415 Edwards, P. M., Aikin, K. C., Dube, W. P., Fry, J. L., Gilman, J. B., de Gouw, J. A., Graus, M. G.,
- 416 Hanisco, T. F., Holloway, J., Hübler, G., Kaiser, J., Keutsch, F. N., Lerner, B. M., Neuman, J. A., Parrish,
- D. D., Peischl, J., Pollack, I. B., Ravishankara, A. R., Roberts, J. M., Ryerson, T. B., Trainer, M., Veres, P.
- 418 R., Wolfe, G. M., Warneke, C., Brown, S. S.: Transition from high- to low-NOx control of night-time
- oxidation in the southeastern US. Nature Geoscience. 10, 490-495. 10.1038/ngeo2976, 2017.
- 420 Estillore, A. D., Hettiyadura, A. P. S., Qin, Z., Leckrone, E., Wombacher, B., Humphry, T., Stone, E.
- 421 A., Grassian, V. H.: Water Uptake and Hygroscopic Growth of Organosulfate Aerosol. Environmental
- 422 Science & Technology. 50, 4259-4268. 10.1021/acs.est.5b05014, 2016.
- Fleming, L. T., Ali, N. N., Blair, S. L., Roveretto, M., George, C., Nizkorodov, S. A.: Formation of
- 424 Light-Absorbing Organosulfates during Evaporation of Secondary Organic Material Extracts in the
- 425 Presence of Sulfuric Acid. ACS Earth and Space Chemistry. 3, 947-957.
- 426 10.1021/acsearthspacechem.9b00036, 2019.
- 427 Fountoukis, C., Nenes, A.: ISORROPIA II: a computationally efficient thermodynamic equilibrium
- 428 model for K+; Ca2+; Mg2+; NH4+; Na+; SO42-; NO3-; Cl-; H2O aerosols. Atmospheric Chemistry and
- 429 Physics. 7, 4639-4659. 10.5194/acp-7-4639-2007, 2007.
- 430 Guenther, A., Karl, T., Harley, P., Wiedinmyer, C., Palmer, P. I., Geron, C.: Estimates of global
- 431 terrestrial isoprene emissions using MEGAN (Model of Emissions of Gases and Aerosols from Nature).
- 432 Atmos. Chem. Phys. 6, 3181-3210. 10.5194/acp-6-3181-2006, 2006.
- 433 Hansen, A. M. K., Hong, J., Raatikainen, T., Kristensen, K., Ylisirniö, A., Virtanen, A., Petäjä, T.,
- 434 Glasius, M., Prisle, N. L.: Hygroscopic properties and cloud condensation nuclei activation of limonene-
- derived organosulfates and their mixtures with ammonium sulfate. Atmos. Chem. Phys. 15, 14071-14089.
- 436 10.5194/acp-15-14071-2015, 2015.





- 437 He, J., Li, L., Li, Y., Huang, M., Zhu, Y., Deng, S.: Synthesis, MS/MS characteristics and quantification
- 438 of six aromatic organosulfates in atmospheric PM2.5. Atmospheric Environment. 290, 119361.
- 439 https://doi.org/10.1016/j.atmosenv.2022.119361, 2022.
- 440 Hettiyadura, A. P. S., Jayarathne, T., Baumann, K., Goldstein, A. H., de Gouw, J. A., Koss, A., Keutsch,
- 441 F. N., Skog, K., Stone, E. A.: Qualitative and quantitative analysis of atmospheric organosulfates in
- Centreville, Alabama. Atmospheric Chemistry and Physics. 17, 1343-1359. 10.5194/acp-17-1343-2017,
- 443 2017.
- Huang, L., Cochran, R. E., Coddens, E. M., Grassian, V. H.: Formation of Organosulfur Compounds
- 445 through Transition Metal Ion-Catalyzed Aqueous Phase Reactions. Environmental Science & Technology
- 446 Letters. 5, 315-321. 10.1021/acs.estlett.8b00225, 2018a.
- 447 Huang, L., Coddens, E. M., Grassian, V. H.: Formation of Organosulfur Compounds from Aqueous
- 448 Phase Reactions of S(IV) with Methacrolein and Methyl Vinyl Ketone in the Presence of Transition Metal
- 449 Ions. ACS Earth and Space Chemistry. 3, 1749-1755. 10.1021/acsearthspacechem.9b00173, 2019.
- 450 Huang, L., Liu, T., Grassian, V. H.: Radical-Initiated Formation of Aromatic Organosulfates and
- 451 Sulfonates in the Aqueous Phase. Environmental Science & Technology. 54, 11857-11864.
- 452 10.1021/acs.est.0c05644, 2020.
- 453 Huang, L., Wang, Y., Zhao, Y., Hu, H., Yang, Y., Wang, Y., Yu, J.-Z., Chen, T., Cheng, Z., Li, C., Li,
- 454 Z., Xiao, H.: Biogenic and Anthropogenic Contributions to Atmospheric Organosulfates in a Typical
- 455 Megacity in Eastern China. Journal of Geophysical Research: Atmospheres. 128, e2023JD038848.
- 456 https://doi.org/10.1029/2023JD038848, 2023a.
- 457 Huang, L., Wang, Y., Zhao, Y., Hu, H., Yang, Y., Wang, Y., Yu, J.-Z., Chen, T., Cheng, Z., Li, C., Li,
- 458 Z., Xiao, H.: Biogenic and Anthropogenic Contributions to Atmospheric Organosulfates in a Typical
- 459 Megacity in Eastern China. 128, e2023JD038848. https://doi.org/10.1029/2023JD038848, 2023b.
- 460 Huang, R. J., Cao, J., Chen, Y., Yang, L., Shen, J., You, Q., Wang, K., Lin, C., Xu, W., Gao, B., Li, Y.,
- Chen, Q., Hoffmann, T., O'Dowd, C. D., Bilde, M., Glasius, M.: Organosulfates in atmospheric aerosol:
- synthesis and quantitative analysis of PM2.5 from Xi'an, northwestern China. Atmos. Meas. Tech. 11, 3447-
- 463 3456. 10.5194/amt-11-3447-2018, 2018b.
- 464 Iinuma, Y., Müller, C., Berndt, T., Böge, O., Claeys, M., Herrmann, H.: Evidence for the Existence of
- 465 Organosulfates from β-Pinene Ozonolysis in Ambient Secondary Organic Aerosol. Environmental Science
- 466 & Technology. 41, 6678-6683. 10.1021/es070938t, 2007a.
- 467 Iinuma, Y., Müller, C., Böge, O., Gnauk, T., Herrmann, H.: The formation of organic sulfate esters in
- 468 the limonene ozonolysis secondary organic aerosol (SOA) under acidic conditions. Atmospheric
- 469 Environment. 41, 5571-5583. https://doi.org/10.1016/j.atmosenv.2007.03.007, 2007b.
- 470 Jiang, H., Cai, J., Feng, X., Chen, Y., Guo, H., Mo, Y., Tang, J., Chen, T., Li, J., Zhang, G.:
- 471 Organosulfur Compounds: A Non-Negligible Component Affecting the Light Absorption of Brown Carbon
- During North China Haze Events. Journal of Geophysical Research: Atmospheres. 130, e2024JD042043.
- 473 <u>https://doi.org/10.1029/2024JD042043</u>, 2025.
- Koss, A. R., Sekimoto, K., Gilman, J. B., Selimovic, V., Coggon, M. M., Zarzana, K. J., Yuan, B.,





- 475 Lerner, B. M., Brown, S. S., Jimenez, J. L., Krechmer, J., Roberts, J. M., Warneke, C., Yokelson, R. J., de
- 476 Gouw, J.: Non-methane organic gas emissions from biomass burning: identification, quantification, and
- 477 emission factors from PTR-ToF during the FIREX 2016 laboratory experiment. Atmos. Chem. Phys. 18,
- 478 3299-3319. 10.5194/acp-18-3299-2018, 2018.
- Le Breton, M., Wang, Y., Hallquist, Å. M., Pathak, R. K., Zheng, J., Yang, Y., Shang, D., Glasius, M.,
- 480 Bannan, T. J., Liu, Q., Chan, C. K., Percival, C. J., Zhu, W., Lou, S., Topping, D., Wang, Y., Yu, J., Lu, K.,
- 481 Guo, S., Hu, M., Hallquist, M.: Online gas- and particle-phase measurements of organosulfates,
- 482 organosulfonates and nitrooxy organosulfates in Beijing utilizing a FIGAERO ToF-CIMS. Atmos. Chem.
- 483 Phys. 18, 10355-10371. 10.5194/acp-18-10355-2018, 2018.
- 484 Li, L., Yang, W., Xie, S., Wu, Y.: Estimations and uncertainty of biogenic volatile organic compound
- 485 emission inventory in China for 2008-2018. Science of The Total Environment. 733, 139301.
- 486 https://doi.org/10.1016/j.scitotenv.2020.139301, 2020.
- 487 Lin, P., Yu, J. Z., Engling, G., Kalberer, M.: Organosulfates in Humic-like Substance Fraction Isolated
- 488 from Aerosols at Seven Locations in East Asia: A Study by Ultra-High-Resolution Mass Spectrometry.
- 489 Environmental Science & Technology. 46, 13118-13127. 10.1021/es303570v, 2012.
- 490 Lin, Y., Han, Y., Li, G., Wang, Q., Zhang, X., Li, Z., Li, L., Prévôt, A. S. H., Cao, J.: Molecular
- 491 Characteristics of Atmospheric Organosulfates During Summer and Winter Seasons in Two Cities of
- 492 Southern and Northern China. Journal of Geophysical Research: Atmospheres. 127, e2022JD036672.
- 493 https://doi.org/10.1029/2022JD036672, 2022.
- Liu, P., Ding, X., Li, B. X., Zhang, Y. Q., Bryant, D. J., Wang, X. M.: Quality assurance and quality
- 495 control of atmospheric organosulfates measured using hydrophilic interaction liquid chromatography
- 496 (HILIC). Atmos. Meas. Tech. 17, 3067-3079. 10.5194/amt-17-3067-2024, 2024.
- 497 Liu, Y., Wu, Z., Wang, Y., Xiao, Y., Gu, F., Zheng, J., Tan, T., Shang, D., Wu, Y., Zeng, L., Hu, M.,
- 498 Bateman, A. P., Martin, S. T.: Submicrometer Particles Are in the Liquid State during Heavy Haze Episodes
- 499 in the Urban Atmosphere of Beijing, China. Environ. Sci. Technol. Lett. 4, 427-432.
- 500 10.1021/acs.estlett.7b00352, 2017.
- 501 Liu, Y. C., Wu, Z. J., Qiu, Y. T., Tian, P., Liu, Q., Chen, Y., Song, M., Hu, M.: Enhanced Nitrate Fraction:
- 502 Enabling Urban Aerosol Particles to Remain in a Liquid State at Reduced Relative Humidity. Geophysical
- 503 Research Letters. 50, e2023GL105505. https://doi.org/10.1029/2023GL105505, 2023.
- 504 Lukács, H., Gelencsér, A., Hoffer, A., Kiss, G., Horváth, K., Hartyáni, Z.: Quantitative assessment of
- 505 organosulfates in size-segregated rural fine aerosol. Atmos. Chem. Phys. 9, 231-238. 10.5194/acp-9-231-
- 506 2009, 2009.
- 507 Ma, J., Ungeheuer, F., Zheng, F., Du, W., Wang, Y., Cai, J., Zhou, Y., Yan, C., Liu, Y., Kulmala, M.,
- 508 Daellenbach, K. R., Vogel, A. L.: Nontarget Screening Exhibits a Seasonal Cycle of PM2.5 Organic Aerosol
- 509 Composition in Beijing. Environmental Science & Technology. 56, 7017-7028. 10.1021/acs.est.1c06905,
- 510 2022.
- 511 Ma, J., Reininger, N., Zhao, C., Döbler, D., Rüdiger, J., Qiu, Y., Ungeheuer, F., Simon, M., D'Angelo,
- 512 L., Breuninger, A., David, J., Bai, Y., Li, Y., Xue, Y., Li, L., Wang, Y., Hildmann, S., Hoffmann, T., Liu, B.,
- 513 Niu, H., Wu, Z., Vogel, A. L.: Unveiling a large fraction of hidden organosulfates in ambient organic aerosol.





- 514 Nature Communications. 16, 4098. 10.1038/s41467-025-59420-y, 2025.
- Meng, X., Wu, Z., Chen, J., Qiu, Y., Zong, T., Song, M., Lee, J., Hu, M.: Particle phase state and
- aerosol liquid water greatly impact secondary aerosol formation: insights into phase transition and its role
- 517 in haze events. Atmospheric Chemistry and Physics. 24, 2399-2414. 10.5194/acp-24-2399-2024, 2024.
- 518 Mutzel, A., Poulain, L., Berndt, T., Iinuma, Y., Rodigast, M., Böge, O., Richters, S., Spindler, G., Sipilä,
- 519 M., Jokinen, T., Kulmala, M., Herrmann, H.: Highly Oxidized Multifunctional Organic Compounds
- 520 Observed in Tropospheric Particles: A Field and Laboratory Study. Environmental Science & Technology.
- 521 49, 7754-7761. 10.1021/acs.est.5b00885, 2015.
- 522 Ohno, P. E., Wang, J., Mahrt, F., Varelas, J. G., Aruffo, E., Ye, J., Qin, Y., Kiland, K. J., Bertram, A.
- 523 K., Thomson, R. J., Martin, S. T.: Gas-Particle Uptake and Hygroscopic Growth by Organosulfate Particles.
- 524 ACS Earth and Space Chemistry. 6, 2481-2490. 10.1021/acsearthspacechem.2c00195, 2022.
- 525 Passananti, M., Kong, L., Shang, J., Dupart, Y., Perrier, S., Chen, J., Donaldson, D. J., George, C.:
- 526 Organosulfate Formation through the Heterogeneous Reaction of Sulfur Dioxide with Unsaturated Fatty
- 527 Acids and Long-Chain Alkenes. Angewandte Chemie International Edition. 55, 10336-10339.
- 528 <u>https://doi.org/10.1002/anie.201605266</u>, 2016.
- Qiu, Y., Liu, Y., Wu, Z., Wang, F., Meng, X., Zhang, Z., Man, R., Huang, D., Wang, H., Gao, Y., Huang,
- 530 C., Hu, M.: Predicting Atmospheric Particle Phase State Using an Explainable Machine Learning Approach
- 531 Based on Particle Rebound Measurements. Environmental Science & Technology. 57, 15055-15064.
- 532 10.1021/acs.est.3c05284, 2023.
- Riva, M., Tomaz, S., Cui, T., Lin, Y.-H., Perraudin, E., Gold, A., Stone, E. A., Villenave, E., Surratt, J.
- 534 D.: Evidence for an Unrecognized Secondary Anthropogenic Source of Organosulfates and Sulfonates:
- 535 Gas-Phase Oxidation of Polycyclic Aromatic Hydrocarbons in the Presence of Sulfate Aerosol.
- 536 Environmental Science & Technology. 49, 6654-6664. 10.1021/acs.est.5b00836, 2015.
- 537 Riva, M., Budisulistiorini, S. H., Zhang, Z., Gold, A., Surratt, J. D.: Chemical characterization of
- 538 secondary organic aerosol constituents from isoprene ozonolysis in the presence of acidic aerosol.
- 539 Atmospheric Environment. 130, 5-13. https://doi.org/10.1016/j.atmosenv.2015.06.027, 2016a.
- Riva, M., Da Silva Barbosa, T., Lin, Y. H., Stone, E. A., Gold, A., Surratt, J. D.: Chemical
- 541 characterization of organosulfates in secondary organic aerosol derived from the photooxidation of alkanes.
- 542 Atmos. Chem. Phys. 16, 11001-11018. 10.5194/acp-16-11001-2016, 2016b.
- 543 Riva, M., Da Silva Barbosa, T., Lin, Y. H., Stone, E. A., Gold, A., Surratt, J. D.: Chemical
- 544 characterization of organosulfates in secondary organic aerosol derived from the photooxidation of alkanes.
- 545 Atmospheric Chemistry and Physics. 16, 11001-11018. 10.5194/acp-16-11001-2016, 2016c.
- Riva, M., Chen, Y., Zhang, Y., Lei, Z., Olson, N. E., Boyer, H. C., Narayan, S., Yee, L. D., Green, H.
- 547 S., Cui, T., Zhang, Z., Baumann, K., Fort, M., Edgerton, E., Budisulistiorini, S. H., Rose, C. A., Ribeiro, I.
- O., e Oliveira, R. L., dos Santos, E. O., Machado, C. M. D., Szopa, S., Zhao, Y., Alves, E. G., de Sá, S. S.,
- Hu, W., Knipping, E. M., Shaw, S. L., Duvoisin Junior, S., de Souza, R. A. F., Palm, B. B., Jimenez, J.-L.,
- Glasius, M., Goldstein, A. H., Pye, H. O. T., Gold, A., Turpin, B. J., Vizuete, W., Martin, S. T., Thornton, J.
- 551 A., Dutcher, C. S., Ault, A. P., Surratt, J. D.: Increasing Isoprene Epoxydiol-to-Inorganic Sulfate Aerosol
- 552 Ratio Results in Extensive Conversion of Inorganic Sulfate to Organosulfur Forms: Implications for





- 553 Aerosol Physicochemical Properties. Environmental Science & Technology. 53, 8682-8694.
- 554 10.1021/acs.est.9b01019, 2019.
- 555 Rudziński, K. J., Gmachowski, L., Kuznietsova, I.: Reactions of isoprene and sulphoxy radical-anions
- 556 a possible source of atmospheric organosulphites and organosulphates. Atmos. Chem. Phys. 9, 2129-2140.
- 557 10.5194/acp-9-2129-2009, 2009.
- 558 Sakulyanontvittaya, T., Guenther, A., Helmig, D., Milford, J., Wiedinmyer, C.: Secondary Organic
- 559 Aerosol from Sesquiterpene and Monoterpene Emissions in the United States. Environmental Science &
- 560 Technology. 42, 8784-8790. 10.1021/es800817r, 2008.
- 561 Song, M., Jeong, R., Kim, D., Qiu, Y., Meng, X., Wu, Z., Zuend, A., Ha, Y., Kim, C., Kim, H., Gaikwad,
- 562 S., Jang, K. S., Lee, J. Y., Ahn, J.: Comparison of Phase States of PM2.5 over Megacities, Seoul and Beijing,
- 563 and Their Implications on Particle Size Distribution. Environmental Science and Technology. 56, 17581-
- 564 17590. 10.1021/acs.est.2c06377, 2022.
- 565 Staudt, S., Kundu, S., Lehmler, H.-J., He, X., Cui, T., Lin, Y.-H., Kristensen, K., Glasius, M., Zhang,
- 566 X., Weber, R. J., Surratt, J. D., Stone, E. A.: Aromatic organosulfates in atmospheric aerosols: Synthesis,
- 567 characterization, and abundance. Atmospheric Environment. 94, 366-373.
- 568 https://doi.org/10.1016/j.atmosenv.2014.05.049, 2014.
- 569 Surratt, J. D., Kroll, J. H., Kleindienst, T. E., Edney, E. O., Claeys, M., Sorooshian, A., Ng, N. L.,
- 570 Offenberg, J. H., Lewandowski, M., Jaoui, M., Flagan, R. C., Seinfeld, J. H.: Evidence for Organosulfates
- 571 in Secondary Organic Aerosol. Environmental Science & Technology. 41, 517-527. 10.1021/es062081q,
- 572 2007.
- 573 Surratt, J. D., Gómez-González, Y., Chan, A. W. H., Vermeylen, R., Shahgholi, M., Kleindienst, T. E.,
- 574 Edney, E. O., Offenberg, J. H., Lewandowski, M., Jaoui, M., Maenhaut, W., Claeys, M., Flagan, R. C.,
- 575 Seinfeld, J. H.: Organosulfate Formation in Biogenic Secondary Organic Aerosol. The Journal of Physical
- 576 Chemistry A. 112, 8345-8378. 10.1021/jp802310p, 2008.
- 577 Tang, J., Li, J., Su, T., Han, Y., Mo, Y., Jiang, H., Cui, M., Jiang, B., Chen, Y., Tang, J., Song, J., Peng,
- 578 P., Zhang, G.: Molecular compositions and optical properties of dissolved brown carbon in biomass burning,
- 579 coal combustion, and vehicle emission aerosols illuminated by excitation-emission matrix spectroscopy
- 580 and Fourier transform ion cyclotron resonance mass spectrometry analysis. Atmos. Chem. Phys. 20, 2513-
- 581 2532. 10.5194/acp-20-2513-2020, 2020.
- Tao, S., Lu, X., Levac, N., Bateman, A. P., Nguyen, T. B., Bones, D. L., Nizkorodov, S. A., Laskin, J.,
- 583 Laskin, A., Yang, X.: Molecular Characterization of Organosulfates in Organic Aerosols from Shanghai and
- 584 Los Angeles Urban Areas by Nanospray-Desorption Electrospray Ionization High-Resolution Mass
- 585 Spectrometry. Environmental Science & Technology. 48, 10993-11001. 10.1021/es5024674, 2014.
- 586 Tolocka, M. P., Turpin, B.: Contribution of Organosulfur Compounds to Organic Aerosol Mass.
- 587 Environmental Science & Technology. 46, 7978-7983. 10.1021/es300651v, 2012.
- Wach, P., Spólnik, G., Rudziński, K. J., Skotak, K., Claeys, M., Danikiewicz, W., Szmigielski, R.:
- 589 Radical oxidation of methyl vinyl ketone and methacrolein in aqueous droplets: Characterization of
- 590 organosulfates and atmospheric implications. Chemosphere. 214, 1-9.
- 591 <u>https://doi.org/10.1016/j.chemosphere.2018.09.026</u>, 2019.





- Wang, G., Zhang, R., Gomez, M. E., Yang, L., Levy Zamora, M., Hu, M., Lin, Y., Peng, J., Guo, S.,
- 593 Meng, J., Li, J., Cheng, C., Hu, T., Ren, Y., Wang, Y., Gao, J., Cao, J., An, Z., Zhou, W., Li, G., Wang, J.,
- Tian, P., Marrero-Ortiz, W., Secrest, J., Du, Z., Zheng, J., Shang, D., Zeng, L., Shao, M., Wang, W., Huang,
- 595 Y., Wang, Y., Zhu, Y., Li, Y., Hu, J., Pan, B., Cai, L., Cheng, Y., Ji, Y., Zhang, F., Rosenfeld, D., Liss, P. S.,
- Duce, R. A., Kolb, C. E., Molina, M. J.: Persistent sulfate formation from London Fog to Chinese haze.
- 597 113, 13630-13635. doi:10.1073/pnas.1616540113, 2016.
- 598 Wang, H., Ma, X., Tan, Z., Wang, H., Chen, X., Chen, S., Gao, Y., Liu, Y., Liu, Y., Yang, X., Yuan, B.,
- 599 Zeng, L., Huang, C., Lu, K., Zhang, Y.: Anthropogenic monoterpenes aggravating ozone pollution. National
- 600 Science Review. 9, nwac103. 10.1093/nsr/nwac103, 2022a.
- Wang, K., Zhang, Y., Huang, R.-J., Wang, M., Ni, H., Kampf, C. J., Cheng, Y., Bilde, M., Glasius, M.,
- 602 Hoffmann, T.: Molecular Characterization and Source Identification of Atmospheric Particulate
- 603 Organosulfates Using Ultrahigh Resolution Mass Spectrometry. Environmental Science & Technology. 53,
- 604 6192-6202. 10.1021/acs.est.9b02628, 2019a.
- Wang, Y., Ren, J., Huang, X. H. H., Tong, R., Yu, J. Z.: Synthesis of Four Monoterpene-Derived
- 606 Organosulfates and Their Quantification in Atmospheric Aerosol Samples. Environmental Science &
- 607 Technology. 51, 6791-6801. 10.1021/acs.est.7b01179, 2017.
- 608 Wang, Y., Hu, M., Guo, S., Wang, Y., Zheng, J., Yang, Y., Zhu, W., Tang, R., Li, X., Liu, Y., Le Breton,
- 609 M., Du, Z., Shang, D., Wu, Y., Wu, Z., Song, Y., Lou, S., Hallquist, M., Yu, J.: The secondary formation of
- organosulfates under interactions between biogenic emissions and anthropogenic pollutants in summer in
- 611 Beijing. Atmospheric Chemistry and Physics. 18, 10693-10713. 10.5194/acp-18-10693-2018, 2018.
- Wang, Y., Ma, Y., Li, X., Kuang, B. Y., Huang, C., Tong, R., Yu, J. Z.: Monoterpene and Sesquiterpene
- 613 α-Hydroxy Organosulfates: Synthesis, MS/MS Characteristics, and Ambient Presence. Environmental
- 614 Science & Technology. 53, 12278-12290. 10.1021/acs.est.9b04703, 2019b.
- 615 Wang, Y., Hu, M., Wang, Y.-C., Li, X., Fang, X., Tang, R., Lu, S., Wu, Y., Guo, S., Wu, Z., Hallquist,
- 616 M., Yu, J. Z.: Comparative Study of Particulate Organosulfates in Contrasting Atmospheric Environments:
- 617 Field Evidence for the Significant Influence of Anthropogenic Sulfate and NOx. Environmental Science &
- 618 Technology Letters. 7, 787-794. 10.1021/acs.estlett.0c00550, 2020.
- 619 Wang, Y., Zhao, Y., Wang, Y., Yu, J. Z., Shao, J., Liu, P., Zhu, W., Cheng, Z., Li, Z., Yan, N., Xiao, H.:
- 620 Organosulfates in atmospheric aerosols in Shanghai, China: seasonal and interannual variability, origin, and
- 621 formation mechanisms. Atmos. Chem. Phys. 21, 2959-2980. 10.5194/acp-21-2959-2021, 2021.
- Wang, Y., Ma, Y., Kuang, B., Lin, P., Liang, Y., Huang, C., Yu, J. Z.: Abundance of organosulfates
- 623 derived from biogenic volatile organic compounds: Seasonal and spatial contrasts at four sites in China.
- 624 Science of The Total Environment. 806, 151275. https://doi.org/10.1016/j.scitotenv.2021.151275, 2022b.
- 625 Wang, Y., Feng, Z., Yuan, Q., Shang, D., Fang, Y., Guo, S., Wu, Z., Zhang, C., Gao, Y., Yao, X., Gao,
- 626 H., Hu, M.: Environmental factors driving the formation of water-soluble organic aerosols: A comparative
- 627 study under contrasting atmospheric conditions. Science of The Total Environment. 866, 161364.
- 628 <u>https://doi.org/10.1016/j.scitotenv.2022.161364</u>, 2023a.
- Wang, Y., Liang, S., Le Breton, M., Wang, Q. Q., Liu, Q., Ho, C. H., Kuang, B. Y., Wu, C., Hallquist,
- 630 M., Tong, R., Yu, J. Z.: Field observations of C2 and C3 organosulfates and insights into their formation





- 631 mechanisms at a suburban site in Hong Kong. Science of The Total Environment. 904, 166851.
- 632 https://doi.org/10.1016/j.scitotenv.2023.166851, 2023b.
- 633 Wei, L., Liu, R., Liao, C., Ouyang, S., Wu, Y., Jiang, B., Chen, D., Zhang, T., Guo, Y., Liu, S. C.: An
- 634 observation-based analysis of atmospheric oxidation capacity in Guangdong, China. Atmospheric
- Environment. 318, 120260. https://doi.org/10.1016/j.atmosenv.2023.120260, 2024.
- 636 Wu, Z., Wang, Y., Tan, T., Zhu, Y., Li, M., Shang, D., Wang, H., Lu, K., Guo, S., Zeng, L., Zhang, Y.:
- 637 Aerosol Liquid Water Driven by Anthropogenic Inorganic Salts: Implying Its Key Role in Haze Formation
- 638 over the North China Plain. Environmental Science & Technology Letters. 5, 160-166.
- 639 10.1021/acs.estlett.8b00021, 2018.
- Ku, L., Yang, Z., Tsona, N. T., Wang, X., George, C., Du, L.: Anthropogenic-Biogenic Interactions at
- 641 Night: Enhanced Formation of Secondary Aerosols and Particulate Nitrogen- and Sulfur-Containing
- 642 Organics from β-Pinene Oxidation. Environmental Science & Technology. 55, 7794-7807.
- 643 10.1021/acs.est.0c07879, 2021.
- Ku, R., Chen, Y., Ng, S. I. M., Zhang, Z., Gold, A., Turpin, B. J., Ault, A. P., Surratt, J. D., Chan, M.
- 645 N.: Formation of Inorganic Sulfate and Volatile Nonsulfated Products from Heterogeneous Hydroxyl
- 646 Radical Oxidation of 2-Methyltetrol Sulfate Aerosols: Mechanisms and Atmospheric Implications.
- Environmental Science & Technology Letters. 11, 968-974. 10.1021/acs.estlett.4c00451, 2024.
- 48 Yang, T., Xu, Y., Ye, Q., Ma, Y. J., Wang, Y. C., Yu, J. Z., Duan, Y. S., Li, C. X., Xiao, H. W., Li, Z. Y.,
- 649 Zhao, Y., Xiao, H. Y.: Spatial and diurnal variations of aerosol organosulfates in summertime Shanghai,
- China: potential influence of photochemical processes and anthropogenic sulfate pollution. Atmos. Chem.
- 651 Phys. 23, 13433-13450. 10.5194/acp-23-13433-2023, 2023.
- 652 Yang, T., Xu, Y., Ma, Y.-J., Wang, Y.-C., Yu, J. Z., Sun, Q.-B., Xiao, H.-W., Xiao, H.-Y., Liu, C.-Q.:
- 653 Field Evidence for Constraints of Nearly Dry and Weakly Acidic Aerosol Conditions on the Formation of
- 654 Organosulfates. Environmental Science & Technology Letters. 11, 981-987. 10.1021/acs.estlett.4c00522,
- 655 2024.
- 4656 Yassine, M. M., Harir, M., Dabek-Zlotorzynska, E., Schmitt-Kopplin, P.: Structural characterization
- 657 of organic aerosol using Fourier transform ion cyclotron resonance mass spectrometry: Aromaticity
- 658 equivalent approach. Rapid Communications in Mass Spectrometry. 28, 2445-2454.
- 659 https://doi.org/10.1002/rcm.7038, 2014.
- 660 Ye, J., Abbatt, J. P. D., Chan, A. W. H.: Novel pathway of SO2 oxidation in the atmosphere: reactions
- with monoterpene ozonolysis intermediates and secondary organic aerosol. Atmos. Chem. Phys. 18, 5549-
- 662 5565. 10.5194/acp-18-5549-2018, 2018.
- Zhang, Y., Chen, Y., Lei, Z., Olson, N. E., Riva, M., Koss, A. R., Zhang, Z., Gold, A., Jayne, J. T.,
- 664 Worsnop, D. R., Onasch, T. B., Kroll, J. H., Turpin, B. J., Ault, A. P., Surratt, J. D.: Joint Impacts of Acidity
- and Viscosity on the Formation of Secondary Organic Aerosol from Isoprene Epoxydiols (IEPOX) in Phase
- Separated Particles. ACS Earth and Space Chemistry. 3, 2646-2658. 10.1021/acsearthspacechem.9b00209,
- 667 2019.
- Zhang, Z., Jiang, J., Lu, B., Meng, X., Herrmann, H., Chen, J., Li, X.: Attributing Increases in Ozone
- 669 to Accelerated Oxidation of Volatile Organic Compounds at Reduced Nitrogen Oxides Concentrations.

https://doi.org/10.5194/egusphere-2025-4549 Preprint. Discussion started: 5 November 2025 © Author(s) 2025. CC BY 4.0 License.





670 PNAS Nexus. 1, pgac266. 10.1093/pnasnexus/pgac266, 2022. 671 Zhao, D., Schmitt, S. H., Wang, M., Acir, I. H., Tillmann, R., Tan, Z., Novelli, A., Fuchs, H., Pullinen, 672 I., Wegener, R., Rohrer, F., Wildt, J., Kiendler-Scharr, A., Wahner, A., Mentel, T. F.: Effects of NOx and 673 SO2 on the secondary organic aerosol formation from photooxidation of α -pinene and limonene. Atmos. 674 Chem. Phys. 18, 1611-1628. 10.5194/acp-18-1611-2018, 2018. 675 Zheng, B., Zhang, Q., Zhang, Y., He, K. B., Wang, K., Zheng, G. J., Duan, F. K., Ma, Y. L., Kimoto, 676 T.: Heterogeneous chemistry: a mechanism missing in current models to explain secondary inorganic 677 aerosol formation during the January 2013 haze episode in North China. Atmos. Chem. Phys. 15, 2031-678 2049. 10.5194/acp-15-2031-2015, 2015. 679